

TE MODE PROPAGATION THROUGH TAPERED CORE LIQUID CRYSTAL OPTICAL FIBERS

P. K. Choudhury

Institute of Microengineering and Nanoelectronics (IMEN)
Universiti Kebangsaan Malaysia
43600 UKM, Bangi, Selangor, Malaysia

W. K. Soon

Faculty of Engineering
Multimedia University
Cyberjaya 63100, Selangor, Malaysia

Abstract—An analysis is presented of a three-layer tapered core liquid crystal optical fiber (TLCF) having the outermost clad section made of radially anisotropic liquid crystal. TE mode propagation through TLCF is demonstrated with maximum distribution of power in the liquid crystal section under the situation that the TLCF core and the inner clad regions are constructed of homogeneous and isotropic dielectric materials. Such a propagation feature is attributed to the radial anisotropy of the liquid crystal outer region, and attracts useful applications of TLCFs in evanescent field optical sensing and other coupling devices primarily used in integrated optics.

1. INTRODUCTION

Complex optical waveguides have been in discussion owing to their versatile technological applications including the areas of nanophotonics and quantum communications [1–12]. Liquid crystal optical fibers (LCFs) also fall in such category, and high optical anisotropic properties of liquid crystals [13, 14] make LCFs attractive for several potential applications [15, 16]. LCFs are generally characterized by the polarization anisotropy — the feature much useful for integrated optic applications [17–19]. As the macroscopic optical properties of liquid crystals can be manipulated by suitably applying

Corresponding author: P. K. Choudhury (pankaj@ukm.my).

external electrical fields [1], LCFs are indispensable in optical sensing too [20, 21]. At this point, it is noteworthy that liquid crystals yield the largest electro-optic effect among other existing materials.

Anisotropy in LCFs may have radial and azimuthal orientations. Reports on LCFs with azimuthal anisotropy [17–19] have appeared in the literature. However, LCFs with radial distributions [22] are less discussed. Thus, the present communication is devoted to the analysis of a three-layer LCF with the outermost cladding made of radially anisotropic liquid crystal — the feature which may be achieved by the capillary action after inserting the liquid crystal into a capillary tube coated with N, N-dimethyl-N-octadecyl-3-aminopropyltrimethoxysilyl chloride [22].

It is well-known that tapered fibers find prominent use in optical sensors and other in-line integrated optic applications [23–27]. As such, a blend of tapered nature and radially anisotropic liquid crystal in fibers — i.e., tapered core liquid crystal optical fibers (TLCFs) — would yield interesting features of the guide. The analysis of such a structure essentially remains much complicated. However, the treatment may be performed by implementing the split-step method wherein a tapered structure is treated in the analogy of a stack of large number of tiny structures with increasing (or decreasing) cross-sections with an end-to-end arrangement [27].

The present communication deals with the investigation of such a three-layer TLCF where the outermost clad is composed of radially anisotropic liquid crystal whereas the core and the inner clad are constructed of dielectric materials. A rigorous analysis is made of the relative distribution of power under the situation when the low order transverse electric (TE) modes are excited in the guide, and the core/clad dimensions are varied. Illustrations are made of the power confinement factors in the three different sections of TLCF against the taper length, and it is observed that the TE modes transport relatively high amount of optical power through the liquid crystal clad — the feature attributed to the tapered nature of the structure as well as the presence of radial anisotropy in the material. It is noticed that, with the increase in input end dimension of TLCF, the distribution of power remains fairly uniform over the taper length — the useful characteristics in fabricating coupling devices and optical sensors based on evanescent field absorption. Though LCFs with radial anisotropies have also been reported before [28], the present communication reports an analytical investigation of a fiber having blend of the features of LCFs and tapered natures (i.e., TLCFs), and the obtained results seem to be rosy in technological applications. As stated above, the use of liquid crystal fibers in optical sensing has

been reported before. However, by making the liquid crystal fiber with tapered structure with the liquid crystal itself in the fiber clad is essentially a new aspect which, to the best of authors' knowledge, not much discussed in the literature. It is observed that a TLCF enhances the sensitivity, as demonstrated in the present paper through rigorous analytical treatments.

2. THEORY

Figure 1 shows the cross-sectional view of a three-layer TLCF with radially anisotropic liquid crystal as the infinitely extended outermost clad where the liquid crystal molecules possess radial orientation with the ordinary and the extraordinary refractive index (RI) values as n_o and n_e , respectively. A comparison of the cases of radial and azimuthal anisotropies of the liquid crystal section makes the situation much clear as Fig. 1(b) illustrates the case when the liquid crystal molecules assume azimuthal anisotropy. Tapered nature of the guide is illustrated in Fig. 2. The other two sections are made of homogeneous, isotropic and non-magnetic materials with the core RI (i.e., n_1) greater than that of the inner cladding (i.e., n_2). We assume that the principal axes of the outer clad coincide with the z -axis (the direction of wave propagation), and the extraordinary principal axis has a radial orientation. The outermost clad will, therefore, have the RI distributions as

$$n_r = n_e \text{ and } n_\phi = n_z \text{ with } n_e > n_1 > n_2 > n_o,$$

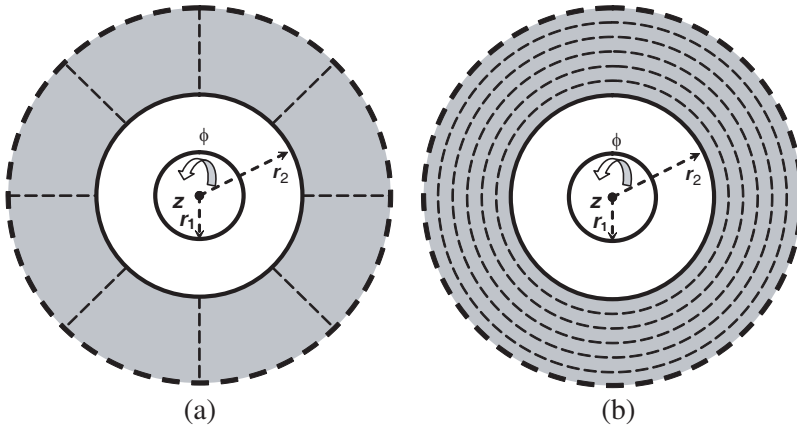


Figure 1. Cross-sectional view of TLCF with the outermost section filled with nematic liquid crystal with (a) radial anisotropy, and (b) azimuthal anisotropy.

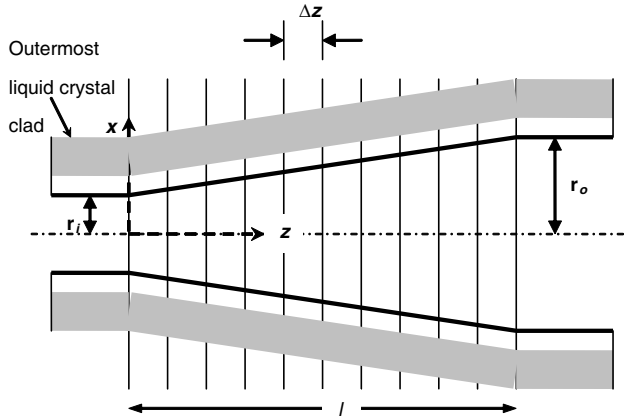


Figure 2. A longitudinal view of TLCF.

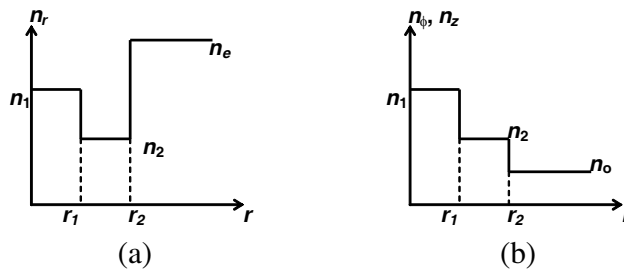


Figure 3. RI distribution pattern.

as shown in Figs. 3(a) and 3(b). Thus, it is to be pointed out that the liquid crystal region of our structure possesses the properties of a positive uniaxial crystal.

For a linear tapered core, we consider the taper radius r as a function of z , defined as

$$r(z) = r_i - \frac{z}{l} (r_i - r_o) \tag{1}$$

with r_i and r_o , respectively, as the radius of the input and the output ends of TLCF, and l as the taper length.

Considering the time t -harmonic and the axis z -harmonic electric/magnetic fields propagating through the TLCF, taper nature of the guide will make the propagation constant β dependent on the cross-sectional dimension. As such, β becomes a function of distance z along the longitudinal direction. We choose the origin of the coordinate system (r, ϕ, z) in a way that when $z = 0$, the cross-sectional radius

is r_i , and at $z = l$, it becomes r_o . However, assuming a small variation in cross-sectional dimension, β may be written in the form of Taylor series expansion [25] as

$$\beta = \beta_0 + \left(\frac{\partial \beta}{\partial z} \right) z \tag{2}$$

where the higher order terms are suppressed as those do not affect the results. In Eq. (2), β_0 is the axial component of the propagation vector at the origin $z = 0$.

Now, the coupled wave propagation equations for the transverse field components may be written as [29, 30]

$$\begin{aligned} \left(\nabla_t^2 + k_0^2 n_r^2 - \beta^2 - \frac{1}{r^2} \right) e_r &= -\frac{2}{r^2} \frac{\partial e_\phi}{\partial \phi} + \left(1 - \frac{n_r^2}{n_z^2} \right) \frac{\partial}{\partial r} \left\{ \frac{1}{r} \frac{\partial}{\partial r} (r e_r) \right\} \\ &+ \left(1 - \frac{n_\phi^2}{n_z^2} \right) \frac{\partial}{\partial r} \left(\frac{1}{r} \frac{\partial e_\phi}{\partial \phi} \right) \end{aligned} \tag{3a}$$

$$\begin{aligned} \left(\nabla_t^2 + k_0^2 n_\phi^2 - \beta^2 - \frac{1}{r^2} \right) e_\phi &= \frac{2}{r^2} \frac{\partial e_r}{\partial \phi} + \frac{1}{r^2} \left\{ \left(1 - \frac{n_r^2}{n_z^2} \right) \frac{\partial}{\partial r} \left(r \frac{\partial e_r}{\partial \phi} \right) \right. \\ &+ \left. \left(1 - \frac{n_\phi^2}{n_z^2} \right) \frac{\partial^2 e_\phi}{\partial \phi^2} \right\} \end{aligned} \tag{3b}$$

where ∇_t^2 is the Laplacian operator, and n_r , n_ϕ and n_z are, respectively, the RI values along the r -, ϕ - and z -directions. Also, k_0 is the free-space propagation constant, and the values of ρ and β are, respectively, governed by Eqs. (1) and (2).

It is to be noted that TE_{mn} , TM_{mn} and hybrid modes in anisotropic waveguides contain all the three electric field components E_r , E_ϕ and E_z . However, there are some special modes which do not contain all the three components of the E -field, and for these, the index profiles in the zero E -field directions are irrelevant to the mode cutoff conditions. We consider the excitation of the low order TE modes (viz. TE_{01}) for which there is only one non-zero transverse E -field component e_ϕ , which is independent of ϕ . Thus, corresponding to this particular mode, we will have $e_r = 0$ and $\partial e_\phi / \partial \phi = 0$. As such, using the above Eq. (3b), it can be shown that the wave equation corresponding to TE modes will have the form

$$\frac{\partial^2 e_\phi}{\partial r^2} + \frac{1}{r} \frac{\partial e_\phi}{\partial r} + \left(k_0^2 n_\phi^2 - \beta^2 - \frac{1}{r^2} \right) e_\phi = 0 \tag{4}$$

where r and β are defined by Eqs. (1) and (2), respectively. On the basis of the solutions to Eq. (4) and Maxwell's field equations, we may

derive the field components in the case of TE₀₁ mode as

$$H_r = -\frac{\beta}{\omega\mu_0} e_\phi \exp\{j(\omega t - \beta z)\} \quad \text{with } H_r = h_r \exp\{j(\omega t - \beta z)\} \quad (5a)$$

$$\text{and } H_z = \frac{j}{\omega\mu_0} \left(\frac{\partial e_\phi}{\partial r} + \frac{e_\phi}{r} \right) \exp\{j(\omega t - \beta z)\}$$

$$\text{with } H_z = h_z \exp\{j(\omega t - \beta z)\} \quad (5b)$$

In these equations, μ_0 is the free-space permeability as we consider all the three mediums as non-magnetic. Using these Eq. (5) and the solutions to Eq. (4), it can be shown that the field components in the different TLCF sections may be deduced as

$$(H_r)_I = -A_{\phi 1} \frac{\beta}{\omega\mu_0} J_1(\gamma_1 r) \exp\{j(\omega t - \beta z)\} \quad (\text{region I}) \quad (6a)$$

$$(H_z)_I = A_{\phi 1} \frac{j}{\omega\mu_0} \left\{ \gamma_1 J_1'(\gamma_1 r) + \frac{1}{r} J_1(\gamma_1 r) \right\} \exp\{j(\omega t - \beta z)\} \quad (\text{region I}) \quad (6b)$$

$$(H_r)_{II} = -\frac{\beta}{\omega\mu_0} \{A_{\phi 2} K_1(\gamma_2 r) + A_{\phi 3} I_1(\gamma_2 r)\} \exp\{j(\omega t - \beta z)\} \quad (\text{region II}) \quad (7a)$$

$$(H_z)_{II} = \frac{j}{\omega\mu_0} \left[A_{\phi 2} \left\{ \gamma_2 K_1'(\gamma_2 r) + \frac{1}{r} K_1(\gamma_2 r) \right\} \right. \\ \left. + A_{\phi 3} \left\{ \gamma_2 I_1'(\gamma_2 r) + \frac{1}{r} I_1(\gamma_2 r) \right\} \right] \exp\{j(\omega t - \beta z)\} \quad (\text{region II}) \quad (7b)$$

$$(H_r)_{III} = -A_{\phi 4} \frac{\beta}{\omega\mu_0} K_1(\gamma_3 r) \exp\{j(\omega t - \beta z)\} \quad (\text{region III}) \quad (8a)$$

$$(H_z)_{III} = A_{\phi 4} \frac{j}{\omega\mu_0} \left\{ \gamma_3 K_1'(\gamma_3 r) + \frac{1}{r} K_1(\gamma_3 r) \right\} \exp\{j(\omega t - \beta z)\}$$

$$(\text{region III}) \quad (8b)$$

In Eqs. (6), (7) and (8), $A_{\phi 1}$, $A_{\phi 2}$, $A_{\phi 3}$ and $A_{\phi 4}$ are the arbitrary constants to be determined by using continuity conditions at the layer interfaces, and the quantities γ_1 , γ_2 and γ_3 are defined as follows:

$$\gamma_1 = \sqrt{n_1^2 k_0^2 - \beta^2} \quad (9a)$$

$$\gamma_2 = \sqrt{\beta^2 - n_2^2 k_0^2} \quad (9b)$$

$$\gamma_3 = \sqrt{\beta^2 - n_o^2 k_0^2} \quad (9c)$$

Also, $J(\cdot)$, $K(\cdot)$ and $I(\cdot)$ are the usual Bessel and the modified Bessel functions, and the prime represents the differentiation with respect to

the argument of the function. At this stage, it must be remembered that r and β are to be considered throughout according to as defined by Eqs. (1) and (2), respectively.

Now, the values of arbitrary constants in Eqs. (6)–(8) can be determined by using the field components as stated in Eqs. (6)–(8), and implementing the conditions of continuity. Finally, after deriving the values of $A_{\phi 2}$, $A_{\phi 3}$ and $A_{\phi 4}$ in terms of $A_{\phi 1}$, and using the above field components, the TE₀₁ mode power [31] transmitted through the different TLCF sections may be expressed as follows:

$$P_C = A_{\phi 1}^2 \frac{\pi}{\omega \mu_0} \left\{ \gamma_1 \int_0^{r_1} r J_1(\gamma_1 r) J_1'(\gamma_1 r) dr + \int_0^{r_1} (J_1(\gamma_1 r))^2 dr \right\} \quad (10)$$

$$P_{IC} = A_{\phi 1}^2 \frac{\pi}{\omega \mu_0} \left[M_1^2 \left\{ \gamma_2 \int_{\rho_1}^{\rho_2} \rho I_1(\gamma_2 \rho) I_1'(\gamma_2 \rho) d\rho + \int_{\rho_1}^{\rho_2} (I_1(\gamma_2 \rho))^2 d\rho \right\} \right. \\ \left. + M_2^2 \left\{ \gamma_2 \int_{r_1}^{r_2} r K_1(\gamma_2 r) K_1'(\gamma_2 r) dr + \int_{r_1}^{r_2} (K_1(\gamma_2 r))^2 dr \right\} \right. \\ \left. + M_1 M_2 \left\{ 2 \int_{r_1}^{r_2} K_1(\gamma_2 r) I_1(\gamma_2 r) dr + \gamma_2 \int_{r_1}^{r_2} r K_1(\gamma_2 r) I_1'(\gamma_2 r) dr \right. \right. \\ \left. \left. + \gamma_2 \int_{r_1}^{r_2} r I_1(\gamma_2 r) K_1'(\gamma_2 r) dr \right\} \right] \quad (11)$$

$$P_{OC} = A_{\phi 1}^2 \frac{\pi}{\omega \mu_0} \left(\frac{M_1 I_1(\gamma_2 r_2) + M_2 K_1(\gamma_2 r_2)}{K_1(\gamma_3 r_2)} \right)^2 \\ \left[\int_{r_2}^{\infty} \{K_1(\gamma_3 r)\}^2 dr + \gamma_3 \int_{r_2}^{\infty} r K_1(\gamma_3 r) K_1'(\gamma_3 r) dr \right] \quad (12)$$

where

$$M_1 = \frac{J_\nu(\gamma_1 r_1) \left\{ \gamma_2 K_\nu'(\gamma_2 r_1) + \frac{1}{r_1} K_\nu(\gamma_2 r_1) \right\}}{I_\nu(\gamma_2 r_1) \left\{ \gamma_2 K_\nu'(\gamma_2 r_1) + \frac{1}{r_1} K_\nu(\gamma_2 r_1) \right\}} \\ - \frac{K_\nu(\gamma_2 r_1) \left\{ \gamma_1 J_\nu'(\gamma_1 r_1) + \frac{1}{r_1} J_\nu(\gamma_1 r_1) \right\}}{K_\nu(\gamma_2 r_1) \left\{ \gamma_2 I_\nu'(\gamma_2 r_1) + \frac{1}{r_1} K_\nu(\gamma_2 r_1) \right\}} \quad (13)$$

and

$$M_2 = \frac{J_\nu(\gamma_1 r_1) \left\{ \gamma_2 I'_\nu(\gamma_2 r_1) + \frac{1}{r_1} K_\nu(\gamma_2 r_1) \right\}}{K_\nu(\gamma_2 r_1) \left\{ \gamma_2 I'_\nu(\gamma_2 r_1) + \frac{1}{r_1} K_\nu(\gamma_2 r_1) \right\}} - \frac{I_\nu(\gamma_2 r_1) \left\{ \gamma_1 J'_\nu(\gamma_1 r_1) + \frac{1}{r_1} J_\nu(\gamma_1 r_1) \right\}}{I_\nu(\gamma_2 r_1) \left\{ \gamma_2 K'_\nu(\gamma_2 r_1) + \frac{1}{r_1} K_\nu(\gamma_2 r_1) \right\}} \quad (14)$$

Above Eqs. (10), (11) and (12), respectively, represent the power transported by the TE₀₁ mode through the TLCHF core, the inner dielectric clad and the outer liquid crystal clad. Further, in Eqs. (10)–(14), r_1 and r_2 represent localized values of the TLCHF core and the inner clad radii, respectively. This is because the fiber structure has a tapered extension (as defined by Eq. (1)) along the longitudinal direction, which cause the radii values to vary. As such, in order to tackle the problem, we implement the split-step method wherein r_1 and r_2 are the radii of a particular step. Also, as stated earlier, the propagation constant β is to be defined by Eq. (2).

The constant A_{ϕ_1} in Eqs. (10), (11) and (12) can be determined by a normalization condition considering the input power. If P_T is the total power transmitted through the LCTF by the TE₀₁ mode, i.e.,

$$P_T = P_C + P_{IC} + P_{OC}, \quad (15)$$

then P_C/P_T ($\equiv \Theta_C$), P_{IC}/P_T ($\equiv \Theta_{ICl}$), and P_{OC}/P_T ($\equiv \Theta_{OCl}$) will, respectively, represent the relative distribution of power (or the power confinement factor) in the fiber core, inner clad and the outer clad of the LCTF.

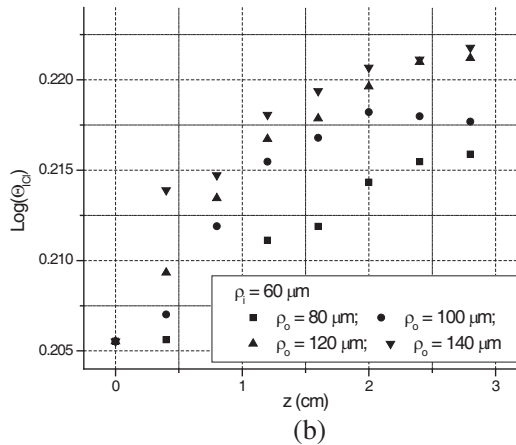
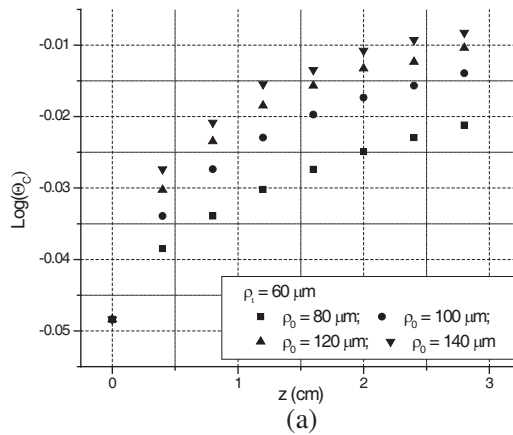
3. RESULTS AND DISCUSSION

We now analyze the characteristics of TLCHF in respect of the relative distribution of power as transported by the TE modes. In our TLCHF structure, the RI values of core and the inner clad are taken as $n_1 = 1.462$ and $n_2 = 1.458$, respectively. Also, for the outermost radially anisotropic liquid crystal clad region, we used nematic liquid crystal as BDH mixture 14616 having the respective ordinary and extraordinary RI values as $n_o = 1.457$ and $n_e = 1.5037$. For simplicity, we considered the modes only with $\nu = 1$ as the azimuthal index. Further, the taper length l in all the computations is taken to be 5 cm and the operating wavelength is kept fixed at 1.55 μm .

It is to be stated at this point that the characteristics of TLCHFs, as reported in the presented communication, may also be illustrated for higher order modes, i.e., $\nu = 2$ or higher. But, in order to reduce

the length of this communication, those results are not incorporated in the discussion part. Corresponding to higher order modes, the authors observed that the amount of power in the different TLCF sections exhibits an increase, however, the trend of variation in the confinement remains almost the same.

It is well-known that TE and TM modes are difficult to separate in the case of isotropic guides. This is owing to the reason that the direction independent RI values yield identical propagation constants and field cutoffs. However, in the case of guides with anisotropic mediums (such as liquid crystals), because of direction-dependent RI values, TE and TM modes will yield different polarization states as well as different values of propagation constants and field cutoffs. However, in the present communication, we concentrate more on the relative distribution of power in the three different sections of TLCF — a guide having anisotropic medium in the outermost section.



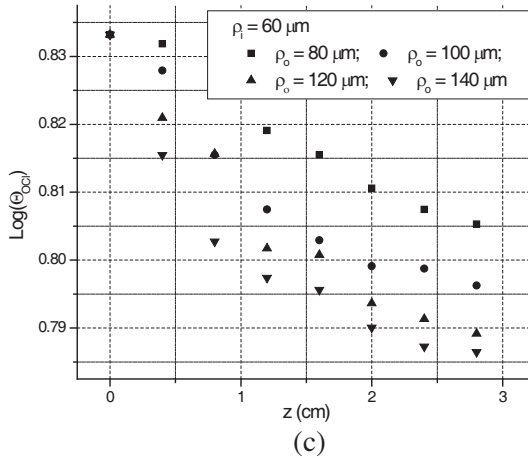
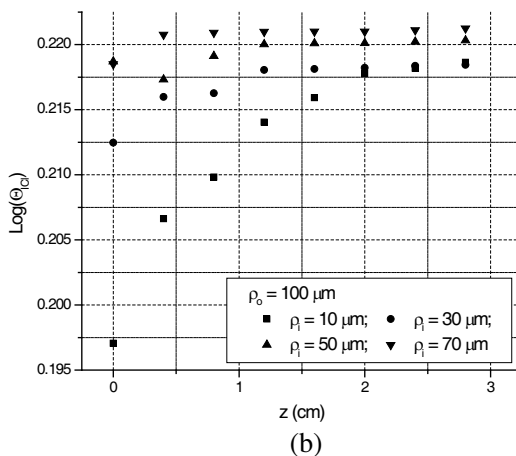
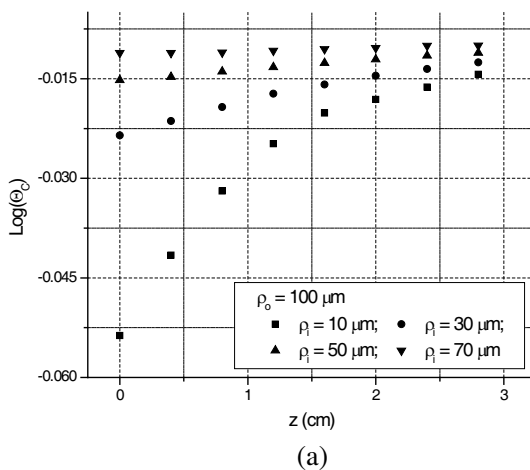


Figure 4. (a) TE mode power confinement in TLCF core. (b) TE mode power confinement in the inner clad of TLCF. (c) TE mode power confinement in the outermost clad of TLCF.

Figure 4 illustrates the situation when the input end dimension of the tapered section is kept fixed whereas the output end dimension is varied. Figs. 4(a), 4(b) and 4(c) correspond to the logarithmic plots of the relative distribution of power in the core, the inner clad and the outer clad, respectively, when the LCTF core radius at the input end is kept fixed as $60 \mu\text{m}$, and that of the output end is varied to be as $80 \mu\text{m}$, $100 \mu\text{m}$, $120 \mu\text{m}$ and $140 \mu\text{m}$. We observe from Figs. 4(a) and 4(b) that, as the taper length is increased towards the longitudinal direction (which is the direction of propagation too), the relative distribution of power increases too. The lowest value of power distribution corresponds to the situation when the outer core radius is taken to be the minimum among the selected values, i.e., $80 \mu\text{m}$. This is because, in this case, lesser amount of power is being carried by the guide as it is having lower dimension. Further, the gradual increase in power distribution is observed owing to the reason that, as the wave propagates across the tapered section, there occurs a continuous increase in the dimension of the guide. It is also noticed that the value of power reaches a kind of saturation in the region near the output end of the tapered section.

Apart from the trend of increasing variation in relative power distribution, another noticeable fact may be observed in Fig. 4(a) that, with all the selected values of TLCF dimensions, a very small amount of power remains confined within the tapered section of the fiber core. Corresponding to the similar values of fiber dimensions

and other operating parameters, the power distribution is seen to be increased in the inner clad (Fig. 4(b)). However, the trend of variation in power remains almost same, as that observed in Fig. 4(a). The power distribution exhibits maximum value in the outermost liquid crystal clad, as can be noticed in Fig. 4(c). Also, the increase in the value of power in this region becomes much pronounced. It is also observed that, with the decrease of power in the fiber core or the inner clad, it simultaneously increases in the outermost liquid crystal clad, indicating thereby as if the power is *leaking off* the fiber core, and propagating through the cladding regions. This phenomenon is attributed to the presence of radially anisotropic liquid crystal medium in the outermost clad region.



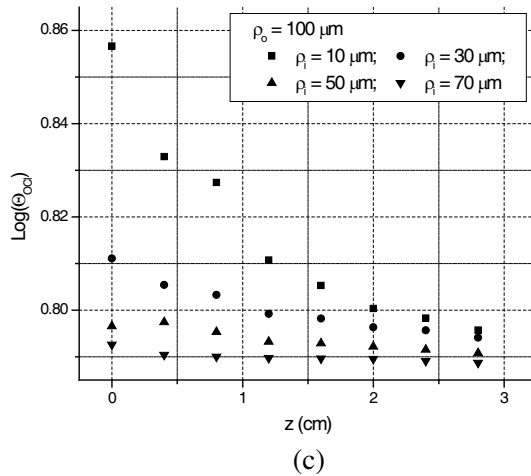


Figure 5. (a) TE mode power confinement in TLCF core. (b) TE mode power confinement in the inner clad of TLCF. (c) TE mode power confinement in the outermost clad of TLCF.

Figure 5 depicts the logarithmic variations of the relative distribution of power when the output dimension of the taper section is kept fixed (output end radius as $100\ \mu\text{m}$) whereas the input dimension is varied. We observe these figures that the variation in power distribution remains maximum with the minimum value of the input core radius ($10\ \mu\text{m}$). With the increase in input dimension, power distribution also becomes uniform without showing much change along the taper length. This is very much obvious as the taper section undergoes maximum variation in dimension along its length with minimum value of radius of the input end.

We observe from Fig. 5(a) that the power distribution remains almost uniform corresponding to the situation when the input core radius is $70\ \mu\text{m}$. The variation in power is seen to be the maximum corresponding to the input core radius as $10\ \mu\text{m}$, and the similar trend is seen in Figs. 5(b) and 5(c) too. Comparison of these three figures yields that the maximum amount of power confinement is observed in Fig. 5(c). This is just the replica of the situation that we observed in Fig. 4(c) — the maximum amount of power is distributed in the outermost clad section of TLCF. This is certainly a new feature observed for TLCFs, and reflects their pronounced usefulness in evanescent field optical sensing. Apart from sensing related applications, the TLCFs would also be demanding in field coupling devices, wherein relatively high amount of power is required to be sustained in the outermost section of the fiber.

4. CONCLUSION

An investigation of the relative distribution of power in TLCFs with radial anisotropy is presented with the emphasis on the power confinement in the tapered section of the guide. The case of TE mode excitation is considered, and it is inferred that a large amount of power remains in the outermost liquid crystal region with substantial difference in the power sustained in the fiber core and the inner dielectric clad. Higher amount of clad power is attributed to the presence of radially anisotropic liquid crystal medium used in TLCF. Further, the tapered structure of guide also plays the role to enhance the property of *power transfer* to the outermost clad. Very large amount of TE mode power in the outermost liquid crystal clad essentially indicates prominent use of such fibers in optical sensing and other integrated optic applications. It is noteworthy that tapered fibers are much promising in the area of field coupling, and the incorporation of liquid crystal section makes the fiber more demanding.

Further work incorporating other propagation modes through TLCFs is in progress, and will be taken up in a future communication.

ACKNOWLEDGMENT

The authors are grateful to one of the anonymous reviewers to critically comment on some issues of the paper, which enhanced the presentation of the text.

REFERENCES

1. Cheng, Q. and T.-J. Cui, "Guided modes and continuous modes in parallel-plate waveguides excited by a line source", *Journal of Electromagnetic Waves and Applications*, Vol. 21, No. 12, 1577–1587, 2007.
2. Mei, Z.-L. and F.-Y. Xu, "A simple, fast and accurate method for calculating cutoff wavelengths for the dominant mode in elliptical waveguide," *Journal of Electromagnetic Waves and Applications*, Vol. 21, No. 3, 367–374, 2007.
3. Kumar, D., P. K. Choudhury, and O. N. Singh II, "Towards the dispersion relations for dielectric optical fibers with helical windings under slow- and fast-wave considerations — A comparative analysis," *Progress In Electromagnetics Research*, PIER 80, 409–420, 2008.
4. Wang, Z.-Y., X.-M. Cheng, X.-Q. He, S.-L. Fan, and W.-Z. Yan, "Photonic crystal narrow filters with negative refractive

- index structural defects,” *Progress In Electromagnetics Research*, PIER 80, 421–430, 2008.
5. Safie, A. H. B. M. and P. K. Choudhury, “On the field patterns of helical clad dielectric optical fibers,” *Progress In Electromagnetics Research*, PIER 91, 69–84, 2009.
 6. Siong, C. C. and P. K. Choudhury, “Propagation characteristics of tapered core helical clad dielectric optical fibers,” *Journal of Electromagnetic Waves and Applications*, Vol. 23, No. 5–6, 663–674, 2009.
 7. Abd-Rahman, F., P. K. Choudhury, D. Kumar, and Z. Yusoff, “An analytical investigation of four-layer dielectric optical fibers with Au nano-coating — A comparison with three-layer optical fibers,” *Progress In Electromagnetics Research*, PIER 90, 269–286, 2009.
 8. Sjoberg, D., “Determination of propagation constants and material data from waveguide measurements,” *Progress In Electromagnetics Research B*, Vol. 12, 163–182, 2009.
 9. Qi, L.-M. and Z. Yang, “Modified plane wave method analysis of dielectric plasma photonic crystal,” *Progress In Electromagnetics Research*, PIER 91, 319–332, 2009.
 10. Watanabe, K. and K. Yasumoto, “Accuracy improvement of the Fourier series expansion method for floquet-mode analysis of photonic crystal waveguides,” *Progress In Electromagnetics Research*, PIER 92, 209–222, 2009.
 11. Lee, H.-S., “A photon modeling method for the characterization of indoor optical wireless communication,” *Progress In Electromagnetics Research*, PIER 92, 121–136, 2009.
 12. Rahman, M. M. and P. K. Choudhury, “Polarized photon generation for the transport of quantum states: A closed-system simulation approach,” *Progress In Electromagnetics Research M*, Vol. 8, 249–261, 2009.
 13. Wu, S.-T. and U. Efron, “Optical properties of thin nematic liquid crystal cells,” *Appl. Phys. Lett.*, Vol. 48, 624–636, 1986.
 14. Green, M. and S. J. Madden, “Low loss nematic liquid crystal cored fiber waveguides,” *Appl. Opt.*, Vol. 28, 5202–5203, 1989.
 15. Veilleux, C., J. Lapierre, and J. Bures, “Liquid-crystal-clad tapered fibers,” *Opt. Lett.*, Vol. 11, 733–735, 1986.
 16. Lin, H., P. P. Muhoray, and M. A. Lee, “Liquid crystalline cores for optical fibers,” *Mol. Cryst. Liq. Cryst.*, Vol. 204, 189–200, 1991.
 17. Sage, I. and D. Chaplin, “Low RI liquid crystals for integrated optics,” *Electron. Lett.*, Vol. 23, 1192–1193, 1987.

18. Kashyap, R., C. S. Winter, and B. K. Nayar, "Polarization desensitized liquid-crystal overlay optical-fiber modulator," *Opt. Lett.*, Vol. 13, 401–403, 1988.
19. Ioannidis, Z. K., I. P. Giles, and C. Bowry, "All-fiber optic intensity modulators using liquid crystals," *Appl. Opt.*, Vol. 30, 328–333, 1991.
20. Yoshino, T., Y. Takahashi, H. Tamura, and N. Ohde, "Some special fibers for distributed sensing of uv light, electric field or strain," *Proc. SPIE*, Vol. 2071, 242–254, 1993.
21. Goldburt, E. S. and P. S. J. Russell, "Electro-optical response of a liquid-crystalline fiber coupler," *Appl. Phys. Lett.*, Vol. 48, 10–12, 1986.
22. Chen, S.-H. and T.-J. Chen, "Observation of mode selection in a radially anisotropic cylindrical waveguide with liquid-crystal cladding," *Appl. Phys. Lett.*, Vol. 64, 1893–1895, 1994.
23. Black, R. J. F. Gonthier, S. Lacroix, and J. D. Love, "Tapered single-mode fibres and devices: I. Adiabaticity criteria," *IEE Proc. J.*, Vol. 138, 343–354, 1991.
24. Ono, K. and H. Osawa, "Excitation characteristics of fundamental mode in tapered slab waveguides with nonlinear cladding," *Electron. Lett.*, Vol. 27, 664–666, 1991.
25. Lim, M. H., S. C. Yeow, P. K. Choudhury, and D. Kumar, "Towards the dispersion characteristics of tapered core dielectric optical fibers," *Journal of Electromagnetic Waves and Applications*, Vol. 20, No. 12, 1597–1609, 2006.
26. Yeow, S. C., M. H. Lim, and P. K. Choudhury, "A rigorous analysis of the distribution of power in plastic clad linear tapered fibers," *Optik*, Vol. 117, 405–410, 2006.
27. Choudhury, P. K. and D. Kumar, "Towards dispersion relations for tapered core dielectric elliptical fibers," *Optik*, Vol. 118, 340–344, 2007.
28. Choudhury, P. K. and T. Yoshino, "On the propagation of power through liquid crystal clad optical fibers," *Proc. SPIE*, Vol. 5560, 380–385, 2004.
29. Snyder, A. W. and F. Rühl, "Single-mode, single-polarization fibers made of birefringent material," *J. Opt. Soc. Am.*, Vol. 73, 1165–1174, 1983.
30. Yijiang, C., "Anisotropic fiber with cylindrical polar axes," *Appl. Phys. B*, Vol. 42, 1–3, 1987.
31. Cherin, A. H., *An Introduction to Optical Fibers*, Chapt. 5, McGraw-Hill, New York, 1987.